Dynamic Manipulability of a Snake-Like Robot with Consideration of Side Force and its Application to Locomotion Control

H. Date[1], Y. Hoshi[2] and M. Sampei[3]

[1,2,3]Tokyo Institute of Technology, Oh-Okayama 2-12-1, Meguro-ku, Tokyo 152-8552, sampei@mei.titech.ac.jp

Abstract

This paper discusses an autonomous locomotion control of a snake-like robot which consists of multiple links with passive wheels and active joints. Such a robot has quite different mechanism in locomotion from that of other locomotion systems. Since the robot has no driving wheel, the locomotability depends on its posture. Thus we utilize a notion of dynamic manipulability to evaluate the locomotability with consideration of the side force wheels. We also propose control method of locomotion control based on this manipulability. Simulation results show a certain periodic winding motion is automatically generated.

1. Introduction

This paper discusses an autonomous locomotion control of a snake-like articulated robot. Such a robot has been attracted attention of many researchers for capability of multiple functions such as grasping and locomotion by varying its shape. Particularly, the mechanism of locomotion is quite different from that of other mobile robots, that is to say, the robot has no driving wheel. There have been proposed several kinds of snake-like robots [3, 4, 5, 7, 9], and this research deals with one of them, an articulated robot with an actuator in each joint and a passive wheel in the middle of each link[7]. It is assumed that the wheels does not sideslip. In some appropriate postures, the robot can locomote using the constraining force of wheels against sideslip arising from actuating the joints. On the contrary, there exists singular postures in which the robot cannot move in some direction. Straight shape or single arc shape is known to be singular postures. Hence the locomotability of the robot largely depends on its posture and it is important to keep some suitable posture to control the locomotion.

Hirose suggested that actuating the joints with sinusoidal inputs generates typical winding motion of natural snakes [3]. A trace of such winding motion is called a serpenoid curve. He developed multi-link robots and applied some control based on the serpenoid curve. In this method, though singular postures can always be avoided, the gait of the robot is fixed beforehand and exact control of the position is difficult. On the contrary, Mita et al. proposed an autonomous locomotion control of the head's position based on Lyapnov function method [7]. In this method, winding motion is generated autonomously in real time and exact position control can be achieved. However, when the number of links is large, amplitude of winding motion tends to decrease, namely, tends to have a singular posture. Hence it is difficult to design a controller satisfying keeping good posture and tracking to a desired trajectory.

Our control objective in this paper is to achieve tracking to a desired trajectory avoiding singular postures without giving any gait beforehand. Since the robot has no driving wheel, locomotability is largely depends on the posture. Thus we utilize a notion of manipulability to evaluate the locomotability. Manipulability is used for a manipulator to evaluate the movability of the end effector [10]. Generally, manipulability is yielded from the relation between the joint torques and the acceleration of the end effector. However, in the case of snake-like robot, such manipulability is not always associated with actual locomotability. When the number of links is large, zigzag winding shape is associated with high manipulability, whereas the actual locomotability is not so good because large amplitude of constraining forces on the wheels are required for locomotion. Then we consider another manipulability for snake-like robot taking the side force on the wheels into consideration. We propose a simple controller capable of trajectory tracking and avoiding singular posture using this manipulability. Simulation results show that the robot spontaneously generates a suitable gait avoiding singular posture.

2. Model of a Snake-Like Robot

In this research, we use an n-link model as a model of snake-like robot [7] (Fig. 1). Each link has a passive wheel which does not sideslip at the middle. Mass, length, moment of inertia of each link are m, l, and J, respectively, and the center of gravity is placed at the

middle of the link; (x_F, y_F) and (x_i, y_i) denote position of the head and position of the i-th link respectively; θ_i is orientation of the i-th link and ϕ_i is relative angle of the $i-1$-th joint; D_{xy} and D_θ are coefficients of the friction of the translational and rotational motion, respectively, of the bottom of each wheel; D_ϕ is the coefficient of the friction in each joint.
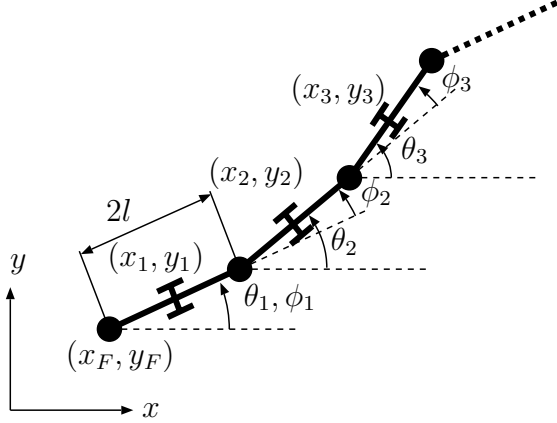
Figure 1: n-link model

2.1. Equation of Motion

Since derivation of equation of motion has previously been shown in the reference [7] in detail, only essential equations are shown. We first ignore the constraint of wheels. Then the equation of motion is similar to that of an n-link manipulator with the exception that no joint nor link is fixed on a base as

$$M(\boldsymbol{\theta})\ddot{\boldsymbol{q}} + C(\dot{\boldsymbol{\theta}}, \boldsymbol{\theta})\dot{\boldsymbol{\theta}} + D(\boldsymbol{\theta})\dot{\boldsymbol{q}} = \begin{bmatrix} E\boldsymbol{\tau} \\ 0 \end{bmatrix}, \quad (1)$$

where $\boldsymbol{\theta} = [\theta_1, \cdots, \theta_n]^T \in R^n$, $\boldsymbol{\tau} \in R^{n-1}$ are joint torques, $\boldsymbol{q} = [\theta_1, \cdots, \theta_n, x_F, y_F]^T \in R^{n+2}$ are generalized coordinates, $M \in R^{n+2 \times n+2}$ is an inertia matrix, $C \in R^{n+2 \times n}$ is a centrifugal coefficient matrix, and $D \in R^{n+2 \times n+2}$ is a frictional coefficient matrix. $E \in R^{n \times n-1}$ satisfies $\boldsymbol{\theta} = E\boldsymbol{\phi}$. Constraint of wheels is expressed as

$$A_\theta \dot{\boldsymbol{\theta}} = B_\theta \dot{\boldsymbol{r}} \quad (2)$$

$$A_\theta = \begin{bmatrix} -l & 0 & \cdots & 0 \\ -2l\cos(\theta_2 - \theta_1) & -l & \cdots & 0 \\ \vdots & & \ddots & \vdots \\ -2l\cos(\theta_n - \theta_1) & \cdots & \cdots & -l \end{bmatrix} \in R^{n \times n}$$

$$B_\theta = \begin{bmatrix} -\sin\theta_1 & \cos\theta_1 \\ \vdots & \vdots \\ -\sin\theta_n & \cos\theta_n \end{bmatrix} \in R^{n \times 2},$$

and this equation yields Pfaffian non-holonomic constraint as

$$\begin{bmatrix} I_n & -F(\boldsymbol{\theta}) \end{bmatrix} \begin{bmatrix} \dot{\boldsymbol{\theta}} \\ \dot{\boldsymbol{r}} \end{bmatrix} = A(\boldsymbol{q})\dot{\boldsymbol{q}} = 0 \quad (3)$$

where $\boldsymbol{r} = [x_F, y_F]^T$ is the position of the head and $F = -A_\theta B_\theta$ is a function of $\boldsymbol{\theta}$. The equation of motion under such constraint[6] can be described by adding a term of constraining force $A(\boldsymbol{q})^T \boldsymbol{\lambda}$ to (1) as

$$M\ddot{\boldsymbol{q}} + C\dot{\boldsymbol{\theta}} + D\dot{\boldsymbol{q}} + \begin{bmatrix} I_n \\ -F^T \end{bmatrix} \boldsymbol{\lambda} = \begin{bmatrix} E\boldsymbol{\tau} \\ 0 \end{bmatrix}, \quad (4)$$

where $\boldsymbol{\lambda} \in R^n$ is the Lagrange's multiplier. By multiplying $\begin{bmatrix} F^T & I_n \end{bmatrix}$ from the left side of (4), we obtain the equation of the head's motion $\boldsymbol{r} = [x_F, y_F]^T$,

$$\tilde{M}\ddot{\boldsymbol{r}} + (\tilde{C} + \tilde{D})\dot{\boldsymbol{r}} = F^T E\boldsymbol{\tau} \quad (5)$$

$$\tilde{M} = [F^T \ I_2]M \begin{bmatrix} F \\ I_2 \end{bmatrix} \in R^{2 \times 2}$$

$$\tilde{C} = [F^T \ I_2]M \begin{bmatrix} F \\ 0 \end{bmatrix} + [F^T \ I_2]CF \in R^{2 \times 2}$$

$$\tilde{D} = [F^T \ I_2]D \begin{bmatrix} F \\ I_2 \end{bmatrix}.$$

The whole motion of the robot is represented in this equation. (5) is a basic equation to discuss manipulability of the snake-like robot.

3. Dynamic Manipulability

In this section, we first show a brief summary of dynamic manipulability used for a manipulator, and then apply it to the snake-like robot. Motion of n-d.o.f manipulator, generally, is given by

$$M(\boldsymbol{\psi})\ddot{\boldsymbol{\psi}} + h(\dot{\boldsymbol{\psi}}, \boldsymbol{\psi}) + g(\boldsymbol{\psi}) = \boldsymbol{\tau}, \quad (6)$$

where $\boldsymbol{\psi} \in R^n$ and $\boldsymbol{\tau} \in R^n$ denote joint angles, joint torques as control inputs, respectively. $M \in R^{n \times n}$ is the moment of inertia which is always nonsingular,

$h \in R^n$ and $g \in R^n$ is inertial force and gravity, respectively. Kinematic constraint due to the joints is expressed as

$$\dot{r} = J(\psi)\dot{\psi} \qquad (7)$$
$$\ddot{r} = J\ddot{\psi} + \dot{J}\dot{\psi}. \qquad (8)$$

Elimination of $\ddot{\psi}$ from (6) and (8), we have

$$\ddot{r} = JM^{-1}[\tau - h - g] + \dot{J}\dot{\psi}. \qquad (9)$$

Normalizing the input by

$$\tau = N v \quad (|v_i| \le 1) \qquad (10)$$
$$N = \mathrm{diag}(\tau_{i\max} - |h_i - g_i|), \qquad (11)$$

we obtain

$$\ddot{r} = JM^{-1}N v + \dot{J}\dot{\theta} \qquad (12)$$

as a relation of normalized input v and the acceleration of the end effector $\ddot{r}$. This implies that the maximum acceleration is characterized by an ellipsoid $JM^{-1}N v$ ($\|v\| \le 1$) as long as $\dot{J}\dot{\psi}$ is relatively small. This ellipsoid is called dynamic manipulability ellipsoid [10]. The larger and the more similar to a sphere the dynamic ellipsoid is, the higher the manipulability is. There have been proposed several measures of manipulability based on this dynamic manipulability ellipsoid as follows:

- the ratio of the length of the ellipsoid's minor axis to that of the major [2]

- the volume of the ellipsoid [10]

- the length of the ellipsoid's minor axis [1]

The choice of these measures varies according to what information of the dynamic ellipsoid is required.

Next, we will apply the notion of manipulability to the snake-like robot. The acceleration of the head caused by the input torques τ is yielded from (5) as

$$\ddot{r} = \tilde{M}F^T E\tau. \qquad (13)$$

The manipulability ellipsoid is characterized by singular values σ_1 and σ_2 of the matrix $\tilde{M}F^T E \in R^{2 \times n-1}$. When the robot has a such shape that the acceleration of head is large with small input torques, the manipulability becomes high. However, zigzag winding shape is associated with high manipulability with this definition of manipulability. With large number of links, shape of high manipulability tends to be straight, namely, the singular posture. Under such posture, the side constraining force on each wheel against sideslip, which is necessary for locomotion, is required to be very large and non-slip assumption may be violated. Therefore, we consider another definition of manipulability taking the side constraining force into consideration.

3.1. Side Constraining Force on Wheels

The constraining force can be calculated from the Lagrange's multiplier λ in (4). First we consider coordinates u_i in direction perpendicular to i-th link. Virtual displacement of each link without constraint of wheels is expressed by

$$\delta u = A_\theta \delta\theta + B_\theta \delta r \qquad (14)$$

where $\delta u = [\delta u_1, \cdots, \delta u_n]^T$, $\delta\theta$, and δr are infinitesimal displacements along each u_i, θ_i, and r, respectively. Let $f = [f_1, \cdots, f_n]^T$ be the constraining forces along u_i axes respectively. Using principle of virtual work, we have

$$f = (A_\theta^T)^{-1}\lambda. \qquad (15)$$

The Lagrange's multiplier λ can be calculated from (4) and (5). Thus we finally obtain

$$f = Y(\theta, \dot{r}) + X(\theta)\tau, \qquad (16)$$

where

$$Y = (A_\theta^T)^{-1}\left\{(M_{11}F + M_{12})\tilde{M}^{-1}[\tilde{C} + \tilde{D}]\right\}$$
$$\quad -M_{11}\dot{F} - (C_1 + D_{11}F - D_{12})\dot{r} \in R^n$$
$$X = (A_\theta^T)^{-1}\left\{I_n - (M_{11}F + M_{12})\tilde{M}^{-1}F^T\right\}E$$
$$\quad \in R^{n \times n-1}.$$

This can be interpreted that $X\tau$ is the side constraining forces cased by input torques τ and Y is that cased by centrifugal force or frictional force.

3.2. Manipulability of a Snake-Like Robot

Ordinary dynamic manipulability becomes high when large acceleration of the head can be obtained with small input torques. On the contrary, in this paper, we consider another manipulability which becomes high when large acceleration of the head can be obtained with small side forces on wheels. From (16), side constraining force caused by input torques τ is given by

$$X\tau = f - Y. \qquad (17)$$

In order to limit the input torques lest each side force f_i exceeds the maximum $f_{i\max}$, we consider a normalized side force $\hat{f}$ ($|\hat{f}_i| \le 1$) and a matrix N such that

$$N = \mathrm{diag}[f_{i\max} - |Y_i|] \quad i = 1, \cdots, n \qquad (18)$$

where Y_i is the i-th element of Y (Fig. 2). Notice that the dimension of the side force f is n whereas the

dimension of the input torques $\boldsymbol{\tau}$ is $n-1$, namely, the matrix X is not square. Hence limited input torque $\hat{\boldsymbol{\tau}}$ is expressed using X^+, pseudo inverse of X, as

$$\hat{\boldsymbol{\tau}} = X^+ N \hat{\boldsymbol{f}}. \qquad (19)$$
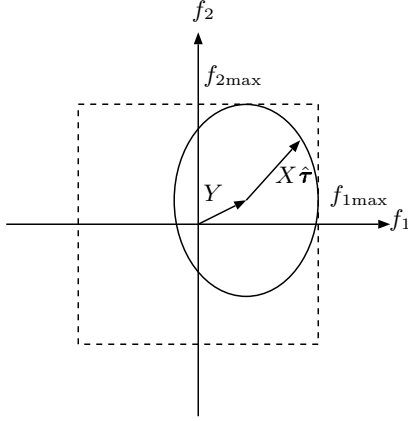
Figure 2: Normalization of side force

The acceleration of the head caused by $\hat{\boldsymbol{\tau}}$ is given by (13) as

$$\ddot{\boldsymbol{r}} = \tilde{M}^{-1} F^T E X^+ N \hat{\boldsymbol{f}}. \qquad (20)$$

When the normalized side force $\hat{\boldsymbol{f}}$ is restricted in a unit sphere, the acceleration of the head $\ddot{\boldsymbol{r}}$ draws an ellipsoid $\tilde{M}^{-1} F^T E X^+ N \hat{\boldsymbol{f}}$ ($\|\hat{\boldsymbol{f}}\| \leq 1$). We regard this ellipsoid as the dynamic manipulability ellipsoid. The singular values σ_1 and σ_2 of the matrix $\tilde{M}^{-1} F^T E X^+ N$ characterize of the dynamic manipulability ellipsoid and smaller one σ_2 is taken as the measure of manipulability here.

Fig. 3-Fig. 6 show distributions of manipulability with sinusoidal oscillation of each joint angle ϕ_i as

$$\phi_i = a \sin\left(\omega t + \frac{2\pi T}{n}(i-1)\right) \qquad (21)$$

where a, ω, and T is the amplitude of oscillation, the frequency, and period of undulation of the body shape. Such curve is known to be a serpenoid curve proposed by Hirose [3].

When the number of links is small, there are little differences between the ordinary manipulability and the proposed one (Fig. 3 and Fig. 4). In this case, both the manipulability becomes high around $T = 1$, where the body has winding shape of 1 period. On
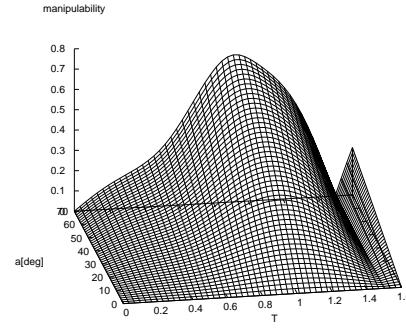
Figure 3: Distribution of ordinary manipulability (4-link)
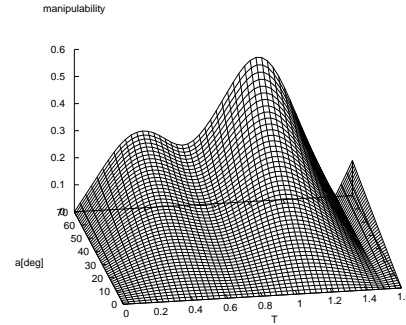
Figure 4: Distribution of proposed manipulability (4-link)
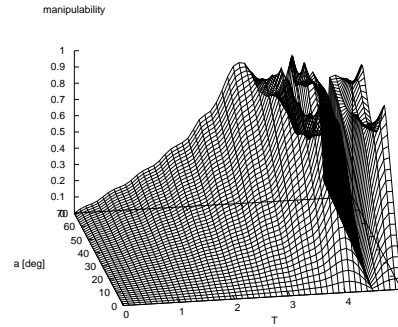
Figure 5: Distribution of ordinary manipulability (10-link)
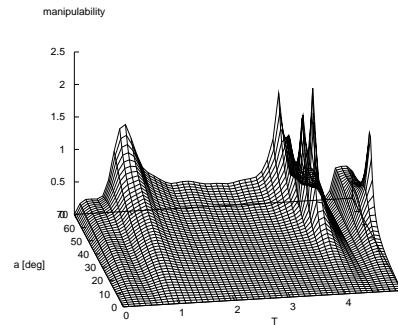
Figure 6: Distribution of ordinary manipulability (10-link)

the contrary, in the case of 10-link, i.e., larger number of links, the proposed manipulability becomes high around $T = 1$ while the ordinary manipulability is high with larger value T (Fig. 5 and Fig. 6). This implies that the proposed manipulability may have essential properties of winding motion of natural snakes.

4. Control of a Snake-Like Robot

The control objective is to achieve tracking to a line avoiding singular posture. Therefore, we propose a controller meeting the following demands.

1. The head of the robot follows a desired trajectory.

2. The posture of the robot should be kept with high manipulability.

Only the position of the head is controlled because the other dynamics is stable zero dynamics. Hence we set two acceleration vectors $\boldsymbol{\alpha}_t$ and $\boldsymbol{\alpha}_m$ of the head to satisfy the preceding requirements (Fig. 7). $\boldsymbol{\alpha}_t$ is an acceleration vector which make the current velocity of the head $\dot{\boldsymbol{r}}$ follow a desired trajectory as

$$\boldsymbol{\alpha}_t = k(\boldsymbol{v}_t - \dot{\boldsymbol{r}}) \qquad (22)$$

where k is a constant and $\boldsymbol{v}_t$ ($\|\boldsymbol{v}_t\| = v$) is a desired velocity toward a desired trajectory. $\boldsymbol{\alpha}_m$ is an acceleration vector which improves the manipulability with constant norm. This vector is searched by a computing. Taking suitably weighed average of these two vectors, the desired acceleration of the head is determined as

$$\boldsymbol{\alpha}_{\text{next}} = w_t \boldsymbol{\alpha}_t + w_m \boldsymbol{\alpha}_m \qquad (23)$$

where w_t and w_m are design parameters.
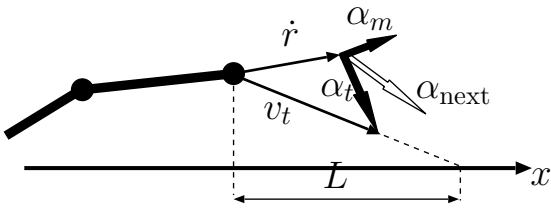
Figure 7: Two acceleration of the head

The input torques which realizes the desired acceleration can be computed from (5) as the inverse dynamics of the head motion as

$$\boldsymbol{\tau} = (F^T E)^+ \left[\tilde{M} \boldsymbol{\alpha}_{\text{next}} + \tilde{C} \dot{\boldsymbol{r}} + \tilde{D} \dot{\boldsymbol{r}} \right] \qquad (24)$$

where $(F^T E)^+$ is the pseudo inverse of $F^T E$.

Fig. 8-Fig. 10 show the simulation results of tracking control to a desired line, x-axis, toward the positive direction. The number of links is 10 and the desired trajectory is x axis. Parameters are given by

$$m = 0.68[\text{kg}], l = 0.5[\text{m}], J = 5.8 \times 10^{-3}[\text{kgm}^2],$$
$$D_{xy} = 1.0 \times 10^{-3}[\text{kg/s}], D_\phi = 0, v = 0.35[\text{m/s}],$$
$$D_\theta = 8.4 \times 10^{-3}[\text{kgm}^2/\text{s}], f_{i\max} = 500[\text{N}]$$

Design parameters are set as

$$k = 1, \; w_t = 1, \; w_m = 0.3 \frac{\|\dot{\boldsymbol{r}}\|}{v}.$$

Fig. 8 and Fig. 9 show trace of the head and body shape at a certain moment. Fig. 8 is the result of tracking control based on the ordinary manipulability. Notice that The amplitude of winding motion is very small. (The vertical scale is magnified 5 times as large as the horizontal scale.) On the contrary, large winding motion can be observed in the results of the control based on the proposed manipulability (Fig. 9).
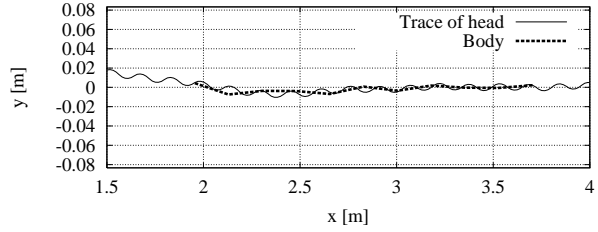
Figure 8: Trace of head; with ordinary manipulability
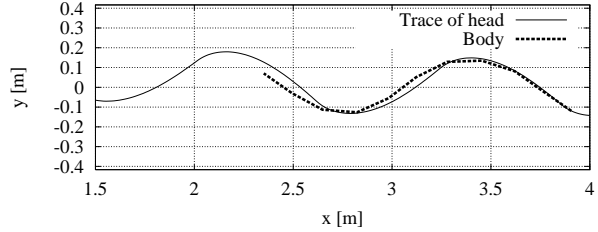
Figure 9: Trace of head; with proposed manipulability

Fig. 11 and Fig. 10 show time evolutions of Euclid norm of input torque $\|\boldsymbol{\tau}\|$ and that of side force $\|\boldsymbol{f}\|$. The norm of input torque is not so different between the ordinary manipulability and the proposed one (Fig. 10). However, the norm of side force in the case of the ordinary manipulability is much larger than that of the proposed manipulability (Fig. 11). From this, we can observe that large winding motion, which can be

seen in the locomotion of natural snakes, saves the side force of wheels.
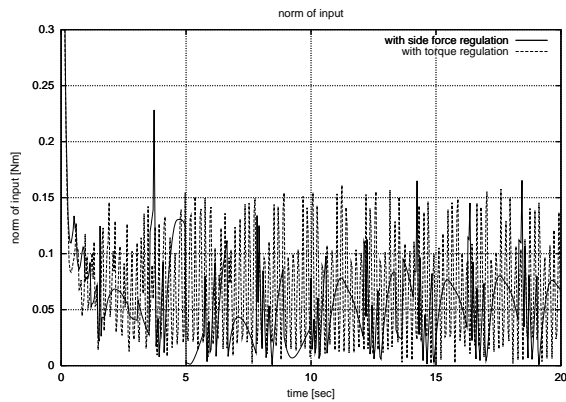
Figure 10: Norm of input
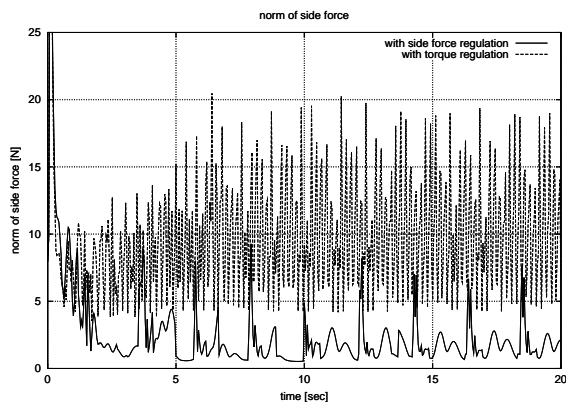
Figure 11: Norm of side force

5. Conclusion

In this paper, dynamic manipulability for a snake-like articulated robot was discussed. As a result, it turned out that such posture that saves the side constraining force on each wheel was associated with large winding shape independent of the number of links. We proposed a simple controller for an autonomous locomotion capable of tracking to a desired trajectory using the proposed manipulability.

Acknowledgement.

References

[1] O. Khabit, 1985, "Dynamic optimazation in manipulator design: The operational space formulation," presented at the ASME Winter Meeting.

[2] K. Kosuge and K. Furuta, 1985, "Kinematic and dynamic analysis of robot arm," *Proc. IEEE Int. Conf. on Robotics and Automation*, pp. 1039–1044.

[3] S. Hirose, 1987, *Biomechanical Engineering*, Kougyou Tyousa Kai.

[4] S. Hirose and A. Morishima, 1990, "Design and Control of a Mobile Robot with an Articulated Body," *The Int. Journal of Robotics Research*, Vol. 9, No. 2, pp. 99–114

[5] G. Migadis and J. Kyriakopoulos, 1997, "Design and forward kinematic analysis of a robotic snake," *IEEE Int. Conf. on Robotics and Automation*, pp. 3493–3498.

[6] R.M. Murray, Z. Li, and S.S. Sastry, 1994, *A Mathematical Introduction to Robotic Manipulation*, CRC Press.

[7] P. Prautsch and T. Mita, 1999, "Control and Analysis of the Gait of Snake Robots," *IEEE Int. Conf. on Conrol Applications*, pp.502–507.

[8] M. Sampei and K. Furuta, 1988, "Robot control in the neighborhood of singular points," *IEEE Trans. on Robotics and Automation*, Vol. 4, No. 3, pp. 303–309.

[9] K. Sarrigeorgidis and K.J. Kyriakopoulos, 1998, "Stabilization and trajectory tracking of a robotic snake," *IEEE Int. Conf. on Robotics and Automation*, pp. 2977–2981.

[10] T. Yoshikawa, 1983, "Analysis and control of manipulators with redundancy," *Proceedings of the First Int. Symposium of Robotics Recearch*, pp. 735–747.